frontiers | Frontiers in Earth Science

TYPE Original Research
PUBLISHED 23 January 2023
DOI 10.3389/feart.2022.1055541

OPEN ACCESS

EDITED BY
Shuai Yin,
Xi'an Shiyou University, China

REVIEWED BY
Caifang Wu,
China University of Mining and Technology, China
Jintong Liang,
Chengdu University of Technology, China

*CORRESPONDENCE
Zhanlei Wang,
28142547@qq.com

SPECIALTY SECTION
This article was submitted to Structural Geology and Tectonics, a section of the journal Frontiers in Earth Science

RECEIVED 27 September 2022
ACCEPTED 22 November 2022
PUBLISHED 23 January 2023

CITATION
Zhou Y, Wang Z, Hu D, Wei Z, Wei X, Liu R, Wang D and Jiang Y (2023), Nanoscale pore characteristics of the Jurassic Dongyuemiao member lacustrine shale, Eastern Sichuan Basin, SW China: Insights from SEM, NMR, LTNA, and MICP experiments. *Front. Earth Sci.* 10:1055541. doi: 10.3389/feart.2022.1055541

Nanoscale pore characteristics of the Jurassic Dongyuemiao member lacustrine shale, Eastern Sichuan Basin, SW China: Insights from SEM, NMR, LTNA, and MICP experiments

Yadong Zhou[1,2,3], Zhanlei Wang[1,2,3]*, Dongfeng Hu[4], Zhihong Wei[4], Xiangfeng Wei[4], Ruobing Liu[4], Daojun Wang[4] and Yuqiang Jiang[1,2,3]

[1]School of Geosciences and Technology, Southwest Petroleum University, Chengdu, China, [2]The Unconventional Reservoir Evaluation Department, PetroChina Key Laboratory of Unconventional Oil and Gas Resources, Chengdu, China, [3]Collaborative Innovation Center of Shale Gas Resources and Environment, Chengdu, China, [4]Sinopec Exploration Company, Chengdu, China

The Jurassic Dongyuemiao Member is the most promising target for lacustrine shale gas exploration in Sichuan Basin. By integrating SEM, NMR, LTNA, and MICP experiments, and other basic measurements, the nanoscale pore category and structure and the corresponding controlling factors of Dongyuemiao lacustrine shale in Eastern Sichuan Basin are studied. The results denote that organic pores comprise primary pores within plant debris and secondary pores within bitumen. Inorganic pores are composed of intraparticle pores within calcite particles, intercrystalline pores between pyrite crystals, and interparticle pores between different minerals. The 4th Section lacustrine shale of Dongyuemiao Member has the best pore structure, exhibiting high organic pore proportion, large amounts of gas adsorption, and parallel plate-shaped pore morphology. Micropores (<2 nm) are the main contributors of the pore volume and surface area of Dongyuemiao lacustrine shale. Moreover, the enrichment of organic matter positively affects the formation of micropores and has no influence on the mesopore–macropore (>2 nm). Quartz does not significantly affect the nanoscale pore formation. The intraparticle pores within calcite particles constitute part of mesopore–macropore but not micropores. Clay minerals are conducive to the formation of micropores but play a negative role in the formation of mesopore–macropore.

KEYWORDS

nanoscale pore, dongyuemiao member, lacustrine shale, pore-size distribution, controlling factors, shale lithofacies

1 Introduction

Organic-rich shale can be deposited in following sedimentary environments: deep shelf, semi-deep to deep lacustrine, estuary bay, and lagoon environment (Zou et al., 2019; Gu et al., 2022a; Gu et al., 2022b; Qiu and He, 2022). In the world, North America has achieved the greatest success in marine shale exploration, followed by China (Zhang et al., 2020a; Zhang et al., 2020b). Several trillion cubic meters-scale shale gas fields, such as Weiyuan, Changning, and Jiaoshiba, have been successively built around the Sichuan Basin to date (Fan et al., 2020; Zhang et al., 2022a; Zhang et al., 2022b; Zhang et al., 2022c; Fan et al., 2022). However, the successful cases of shale gas exploration and development in China are limited to the Silurian marine shale in the Sichuan Basin and its surrounding areas (Zhang et al., 2019; Li, 2022; Li et al., 2022). With the advancement of exploration and development, alternative shale gas exploration targets need to be found (Shu et al., 2021; Sun et al., 2022; Wang et al., 2022). To date, studies on the exploration potential of lacustrine shale gas have been conducted in the Jurassic Da'anzhai Member of Sichuan Basin, Triassic Yanchang Formation in Ordos Basin, Shahejie Formation of Bohai Bay Basin, Cretaceous Shahai and Jiufotang Formation in Fuxin Basin, and the Cretaceous Qingshankou Formation of Songliao Basin (Chen et al., 2018). Results have shown that the organic matter maturity of lacustrine shale is generally low, and the R_o value is mainly in the range of 0.6%–1.1% (Wang et al., 2015; Yang and Zou, 2019), which is mostly in the oil generation stage. Inorganic pores are well-developed, but organic pores are not developed due to low maturity and oil-prone kerogens (Xu et al., 2017; Chen et al., 2018; Han et al., 2021). The organic matter maturity of the Jurassic Dongyuemiao Member lacustrine shale in Sichuan Basin is relatively high. In terms of organic matter maturity, the lacustrine shale in Dongyuemiao Member has been in a stage of high maturity evolution, which is conducive to the development of organic pores (Shu et al., 2021; Liu et al., 2021). In 2018, lacustrine shale gas reservoirs of the Dongyuemiao Member were discovered through Well FY10HF in Eastern Sichuan Basin. However, few studies have been conducted on pore development in Dongyuemiao Member, and thus, its development is poorly understood. Liu et al. (2021) proposed that in the Dongyuemiao lacustrine shale of Northern Sichuan, only inorganic pores are developed and organic pores are not basically developed. However, Shu et al. (2021) proposed contrasting views, proposing that the pore types of shale in the Dongyuemiao shale are diverse and that inorganic pores, organic pores, and fractures are all developed.

The nanoscale pore structure has been identified as one of the most important mechanisms to affect hydrocarbon recovery from unconventional shale reservoirs (Chen et al., 2018; Han et al., 2021; Wang et al., 2022). Understanding nanoscale pore structure and its controlling factors is beneficial for shale reservoir evaluation. A large number of pore structure studies have been carried out on marine shale and found that nanoscale pore structure is strongly affected by mineral composition and organic matter abundance (Li et al., 2016; Jia et al., 2020). However, due to the huge difference in sediment composition, mineral composition and organic matter abundance between lacustrine shale and marine shale (Yang et al., 2019; Li et al., 2021; Wei et al., 2021), the previous results of marine shale cannot be directly applied to lacustrine shale.

Scanning electron microscopy (SEM), Mercury injection capillary pressure (MICP), low-temperature N2 adsorption (LTNA), and nuclear magnetic resonance (NMR) have been widely used to illustrate pore structure parameters and their controlling factors. The above mentioned methods are employed in this study to 1) reveal the dominant reservoir space type of the Dongyuemiao lacustrine shale reservoir, 2) demonstrate the pore structure of the Dongyuemiao lacustrine shale reservoir, and 3) quantitatively discuss the correlation between different parameters and then reveal the main factors controlling the pore structure.

2 Geological setting

Sichuan Basin is a typical craton basin in the western part of the Upper Yangtze Block (Figure 1A), and the basin area is about 260,000 km^2. The study area, with an area of 4.2×10^3 km^2, is located in the Eastern Sichuan Basin (Figure 1B). In the Early-Middle Jurassic, most areas of the Sichuan Basin were dominated by shore-shallow lake, semi-deep lake and deep lake facies, and they experienced four lake transgressions during this period. Organic-rich shale is thought to develop in semi-deep lake and deep lake facies controlled by anoxic condition (Shu et al., 2021; Peng et al., 2022). From the bottom to the top, four sets of organic-rich shales are formed in the Zhenzhuchong Member, Dongyuemiao Member, Da'anzhai Member, and Lianggaoshan 2nd Member, respectively. The Dongyuemiao Member comprises three submembers: 1st Submember, 2nd Submember, and 3rd Submember. The 1st Submember can be subdivided into four sections: 1st, 2nd, 3rd, and 4th Sections (Figure 1C). Except for the 2nd Submember, the other intervals mainly constitute shale. The total organic carbon content (TOC) of shale is mainly distributed in the range of 0.5%–2.0%, and the average value of TOC is greater than 1% (Liu et al., 2021). The organic matter type of the shale is mainly Type II and locally developed Type III, and the vitrinite reflectance (R_o) is mostly greater than 1.2%. Thus, it has entered the stage of high maturity evolution and is dominated by gas generation.

3 Sample and method

A total of 120 core samples of Dongyuemiao Member lacustrine shale were collected from studied wells for thin-section analysis, X-ray diffraction and TOC measurement. The experimental test site is the SINOPEC Wuxi Research

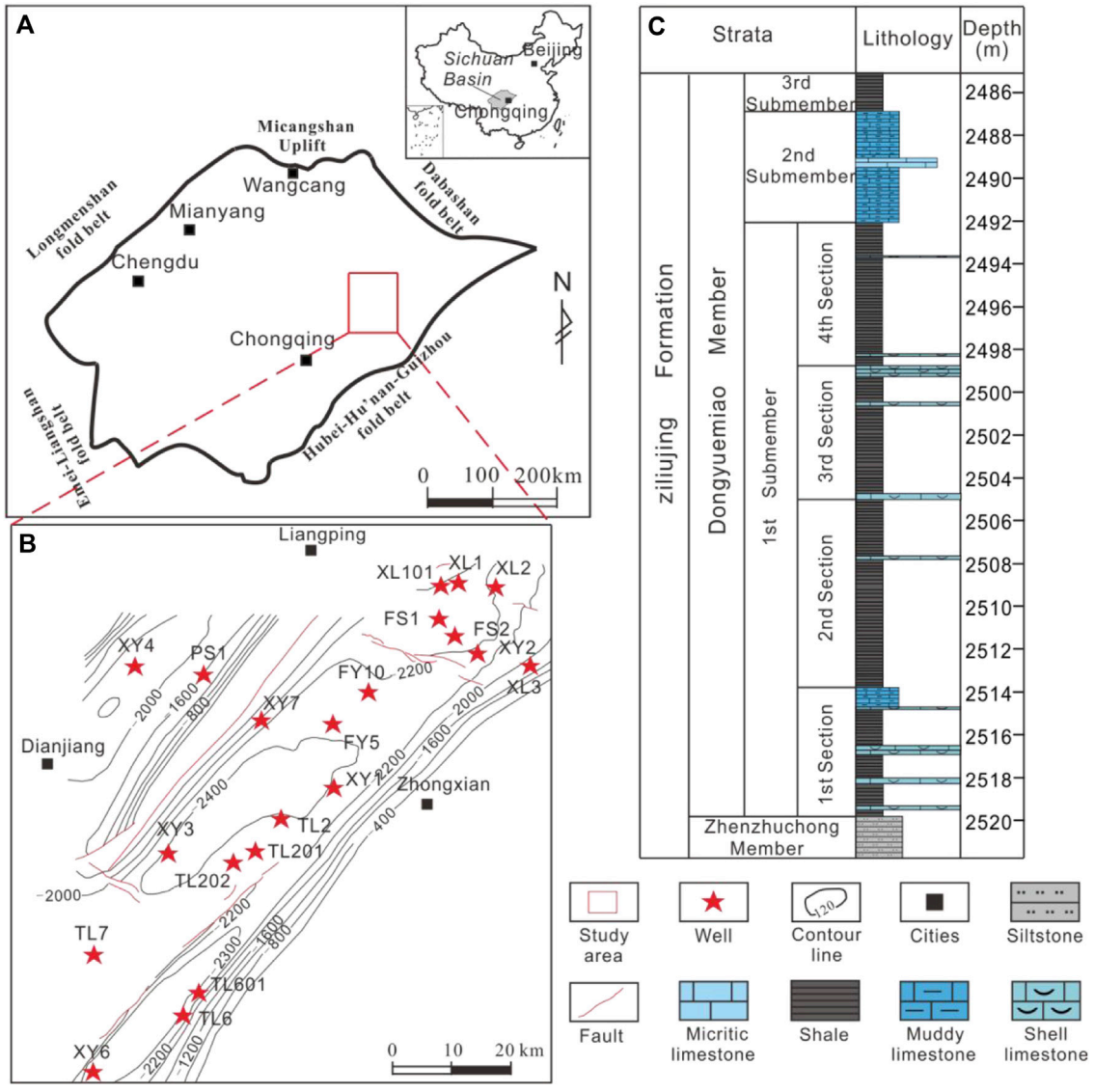

FIGURE 1
(A) Location of the study area in Eastern Sichuan Basin. **(B)** Distribution map showing the burial depth of Jurassic Dongyuemiao Member and studied wells. **(C)** Generalized stratigraphy of Jurassic Dongyuemiao Member in the study area.

Institute of Petroleum Geology. The whole-rock and clay mineral X-ray diffraction measurement was carried out using a German Bruker D8 Advance X-ray diffractometer. TOC measurement was carried out through a LECO CS230 Series Carbon and Sulfur Analyzer. NMR analysis was performed on 24 core-plug shale samples in both the dry and saturated fluid states (including n-dodecane and brine) using a c12-010V low-field NMR device manufactured at the Collaborative Innovation Center of Shale Gas Resources and Environment in Chengdu. Mercury intrusion was measured using a Quantachrome Poremaster. Samples were prepared with an approximate size of 20 × 20 mm^2 and weighed out to 10–20 g, and then, the samples were dried at 110°C for at least 24 h under vacuum in an oven. The Mercury injection pressure ranged from 0 to 215 Mpa in this experiment. The remaining samples were divided into three parts for maceral identification after kerogen extraction, SEM, and LTNA. For LTNA, the samples were crushed into 60–80 mesh, dried in an oven at 110°C for 12 h, and then placed in an Autosorb-IQ3 specific surface and a pore size distribution analyzer (Cantor Company, United States). The pretreatment was completed by degassing at 110°C for 12 h in the vacuum condition, and then nitrogen carbon adsorption was carried out. After the

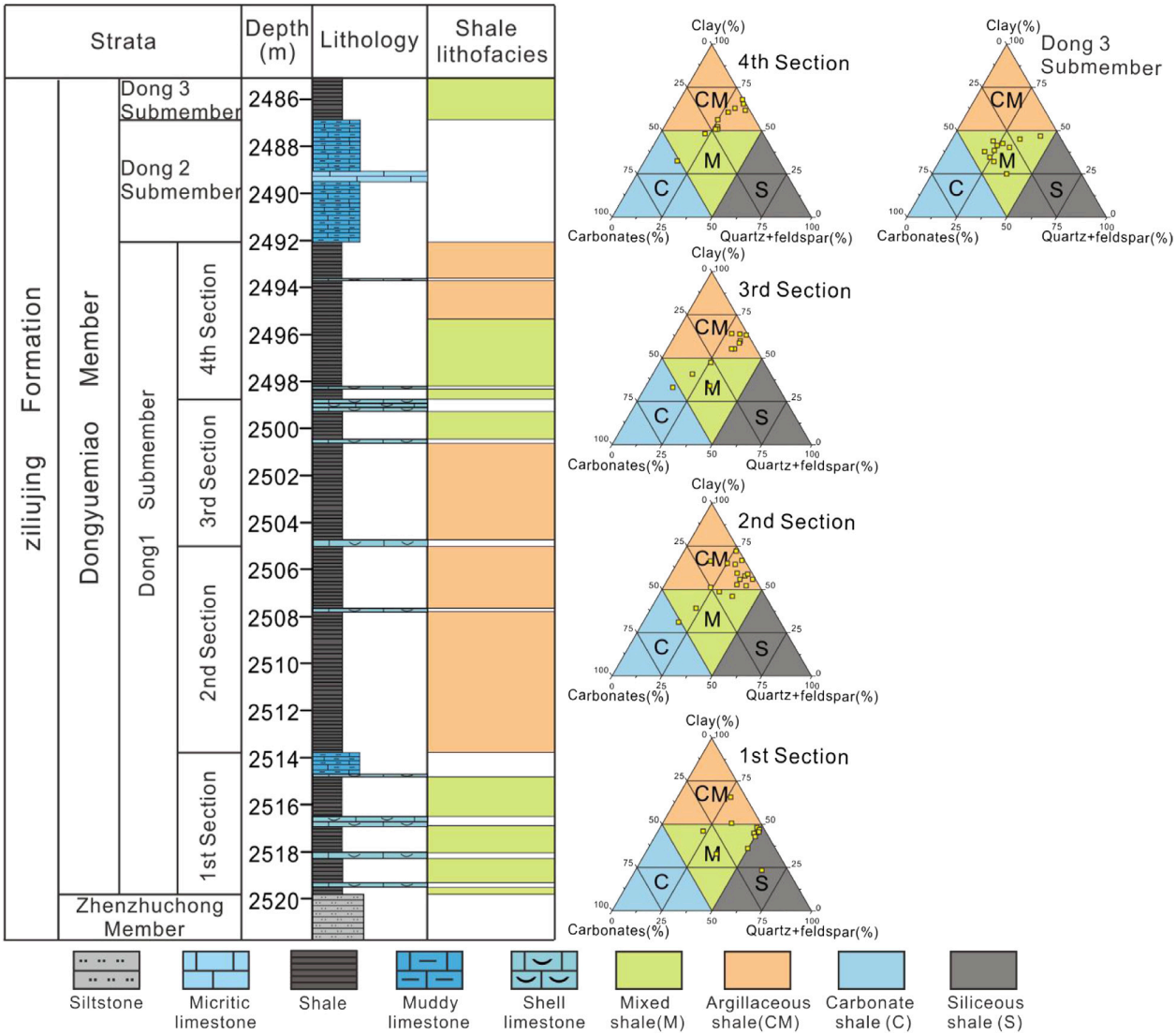

FIGURE 2
Shale lithofacies classification and vertical distribution of the Jurassic Dongyuemiao lacustrine shale in Eastern Sichuan Basin (based on Well XY4).

experiment, the Brunauer–Emmett–Teller (BET) model was used to calculate the specific surface area, and the Barrett–Joyner–Halenda (BJH) model was employed to obtain the pore size distribution and volume. The reservoir space classification is based on schemes proposed by Loucks et al. (2012). The pore size was divided into three categories according to the pore size classification scheme (Rouquerol et al., 1994), namely micropores (<2 nm), mesopores (2nm–50 nm), and macropores (>50 nm). Hysteresis loops were observed at the relative pressure (P/P_O) of about 0.5 in the adsorption–desorption curves, signifying the presence of great differences in the pore size and pore morphology among shale samples that cause such adsorption behaviors at this pressure. This relative pressure was set as the threshold to divide the samples into two groups (Wang et al., 2022). The first group with P/P_O=0-0.5 is subjected to the monolayer-multilayer adsorption process controlled by van der Waals force, while the second group with P/P_O=0.5-1.0 experiences the capillary condensation adsorption process controlled by surface tension (Sun et al., 2015; Wang et al., 2015). Herein, the Frenkel–Halsey–Hill model is used to separately determine the fractal dimensions of these two groups of samples, which are denoted as D_2 and D_1 for the first and second groups, respectively.

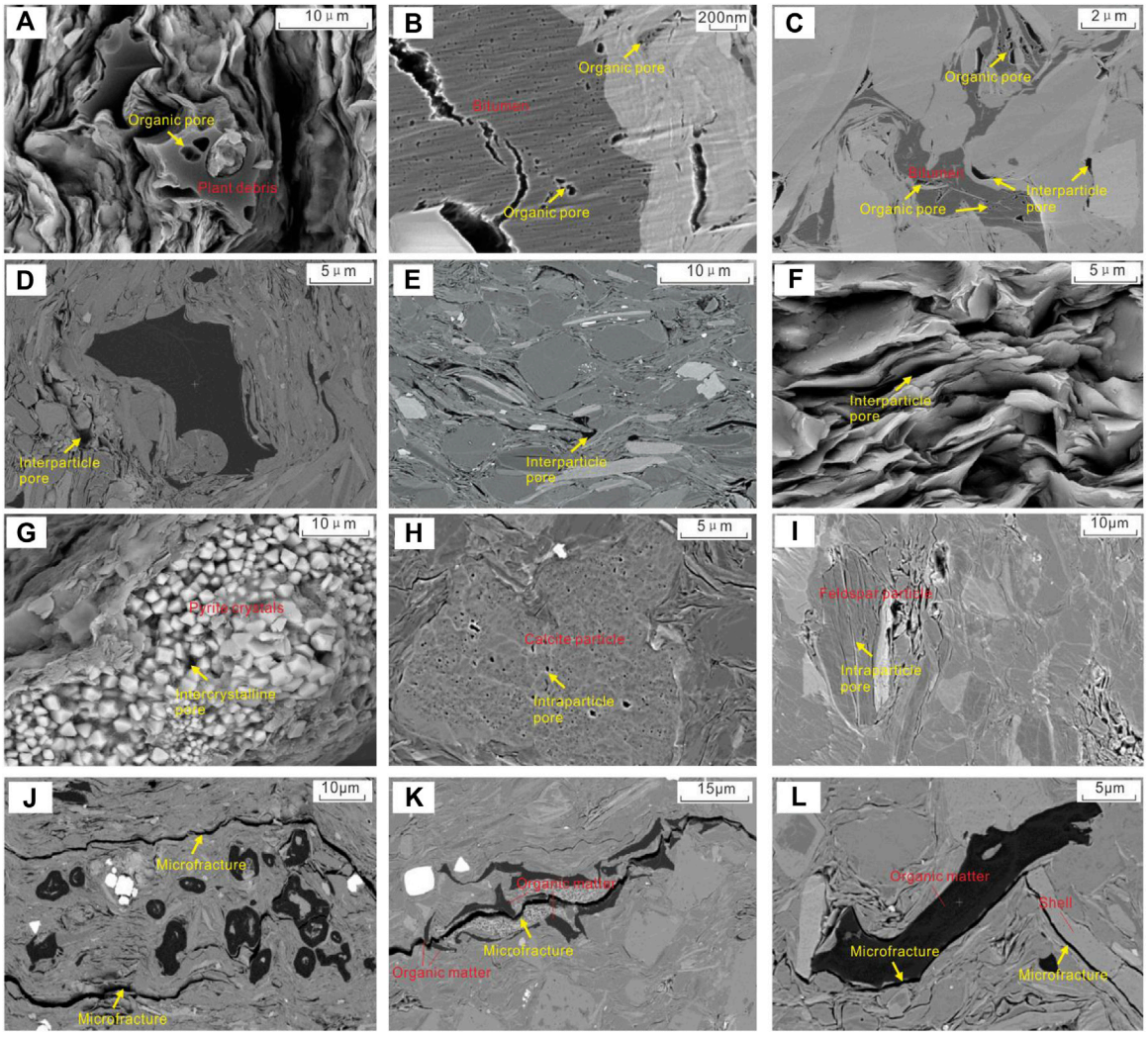

FIGURE 3
FE-SEM images of reservoir spaces in the Jurassic Dongyuemiao lacustrine shale in Eastern Sichuan Basin. **(A)** Primary organic pore in plant debris, Well XY3, 2959 m; **(B)** Abundant organic pore in bitumen, Well FY10, 2,766.46 m; **(C)** Organic pore between bitumen and mineral particles, Well FY10, 2,800.97 m; **(D)** Interparticle pores between mineral particles, Well TL601, 2,743.5 m; **(E)** Interparticle pores between mineral particles, Well TL601, 2,755.13 m; **(F)** Interparticle pores between clay mineral, Well XY3, 2,953.22 m; **(G)** Intercrystalline pores between pyrite crystals, Well XY3, 2,935.1 m; **(H)** Abundant intraparticle pores in calcite particle, Well TL601, 2,731.58 m; **(I)** Intraparticle pores in feldspar particle, Well TL601, 2,728.05 m; **(J)** Microfracture, Well TL601, 2,750.21 m; **(K)** Microfracture dislocating organic matter, Well TL601, 2,731.58m; **(L)** Microfractures around organic matter and mineral particles, Well TL601, 2,731.58 m.

4 Results

4.1 Lithofacies classification

Based on previous lithofacies classification schemes (Jia et al., 2020), the clay, carbonate, and silicon (quartz and feldspar) mineral contents of each shale sample were plotted onto a ternary diagram (Figure 2). The contents of clay minerals, siliceous minerals (quartz + feldspar) and carbonate minerals are regarded as three end-members to divide the mineral lithofacies: argillaceous shale lithofacies (CM) with clay mineral mass fraction >50%; mixed shale lithofacies (M) with clay minerals, siliceous minerals and carbonate minerals <50%. According to the classification results, the 1st and 2nd Sections are composed of mixed shale lithofacies (M) and argillaceous shale lithofacies (CM). In comparison, the 3rd Section predominantly constitutes argillaceous shale lithofacies (CM). While the bottom-to-top lithofacies of the 4th Section is mixed shale lithofacies (M) and argillaceous shale lithofacies (CM) (Figure 2).

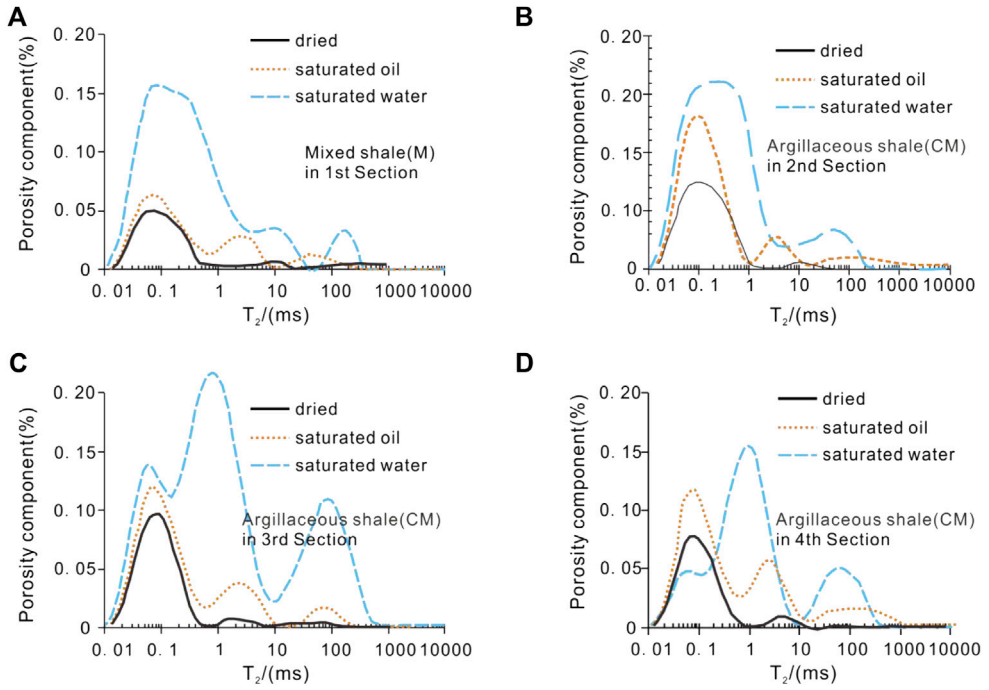

FIGURE 4
NMR T_2 spectra of different shale lithofacies under different states for the Jurassic Dongyuemiao lacustrine shale in Eastern Sichuan Basin.

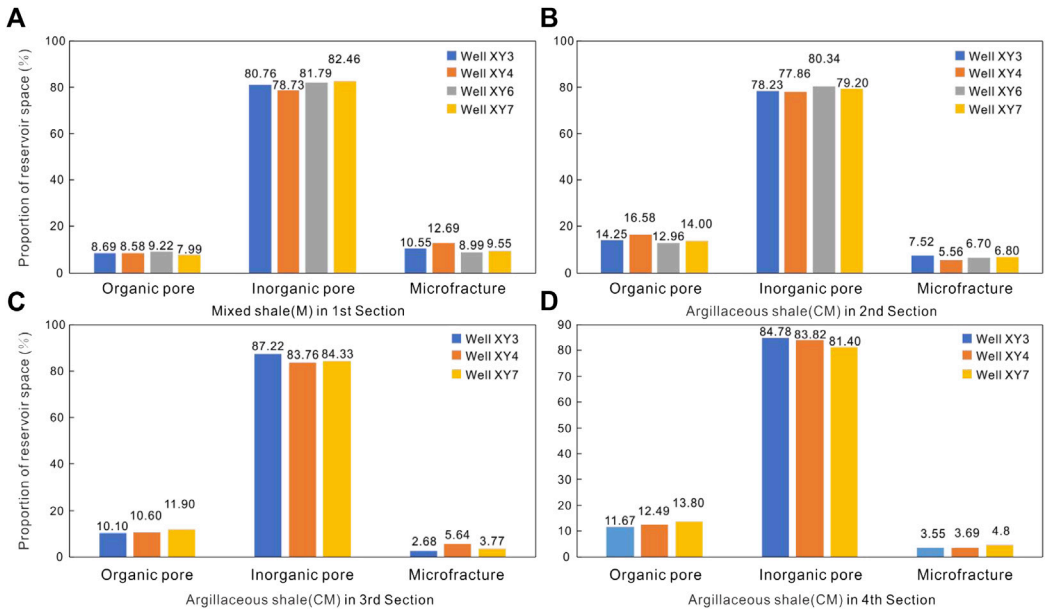

FIGURE 5
Histogram showing proportion of reservoir spaces in different shale lithofacies for the Jurassic Dongyuemiao lacustrine shale in Eastern Sichuan Basin.

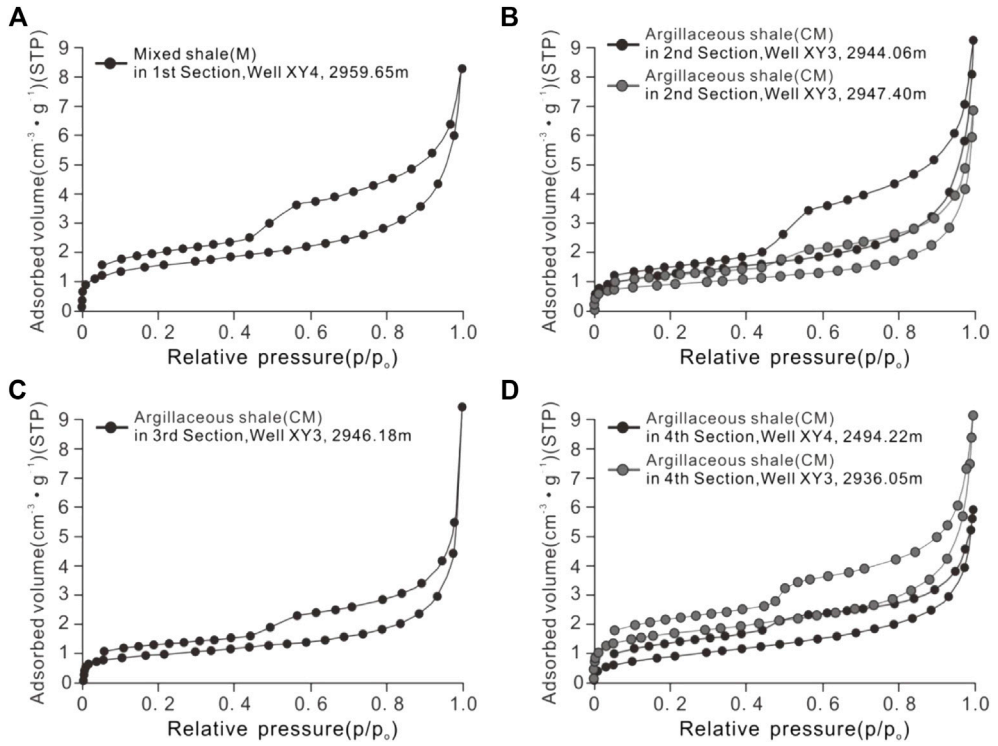

FIGURE 6
The LTNA characteristics of different shale lithofacies for the Jurassic Dongyuemiao lacustrine shale in Eastern Sichuan Basin.

4.2 Reservoir space morphology and proportion

4.2.1 Organic pores

The organic matter of Dongyuemiao lacustrine shale is in the high maturity stage (R_o = ~1.64%). A small number of primary organic pores can be observed inside the plant debris (Figure 3A). Numerous nanoscale organic pores can be observed inside the bitumen (Figure 3B). As an important part of shale pore system, organic pores within bitumen are formed in the process of shale hydrocarbon generation and evolution, which are the traces of shale gas generation diffusion and accumulation. Additionally, organic pores are observed between bitumen and its surrounding mineral particles (Figure 3C). Such organic pores are formed by the shrinkage of organic matter itself after hydrocarbon expulsion.

4.2.2 Interparticle and intercrystalline pores

The migration of sediments in the paleoenvironment will yield considerable micro sedimentary structures, and incomplete cementation between various particles will afford interparticle pores (Han et al., 2013). The interparticle pores of Dongyuemiao lacustrine shale mainly exist between different mineral particles (Figure 3D), such as clay minerals (Figure 3E), quartz, pyrite, and siderite. The size of interparticle pores is controlled by the size of mineral particles and the degree of compaction (Figure 3F). The larger the mineral particles, the larger the interparticle pores, and the greater the buried depth, the less the interparticle pores. In addition to interparticle pores, a large number of interparticle pores develop between pyrite crystals (Figure 3G). However, since the content of pyrite is generally less than 5%, the development frequency of interparticle pores is very low.

4.2.3 Intraparticle pores

The intraparticle pores of Dongyuemiao lacustrine shale mainly formed due to the dissolution of calcite and feldspar particles (Figure 3H). Intraparticle pores are well developed within each calcite and feldspar particle (Figure 3I). In terms of the pore size, the intraparticle pores of Dongyuemiao lacustrine shale belong to the mesopore–macropore, but the development frequency of such pores is generally low.

4.2.4 Microfracture

The microfractures developed in the Dongyuemiao lacustrine shale can be classified as structural or non-structural microfractures. Structural fractures are usually characterized by a stable extension direction with few branches and a large length (Figure 3J). Locally, the

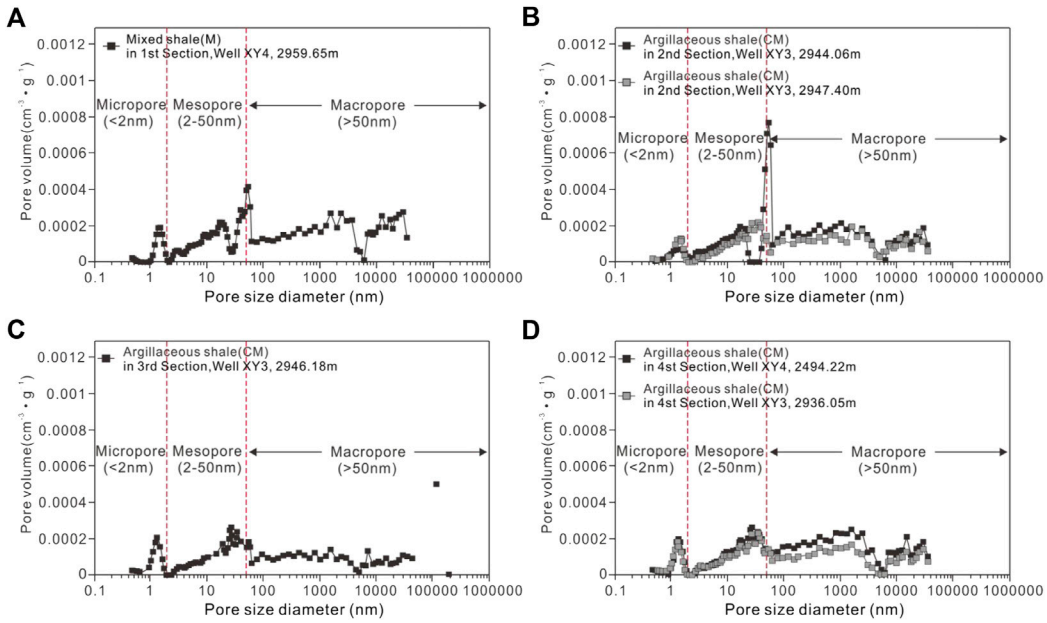

FIGURE 7
Pore-size distribution of different shale lithofacies with MICP and LTNA for the Jurassic Dongyuemiao lacustrine shale in Eastern Sichuan Basin.

microfracture dislocates the organic matter or mineral particles (Figure 3K). In comparison, non-structural fractures have the characteristics of short extension around the edges of the organic matter or the other mineral particles including the shell (Figure 3L).

4.2.5 Proportion of different reservoir spaces

Organic pores are generally lipophilic, while inorganic pores are mostly hydrophilic (Tinni et al., 2014; Li et al., 2016). Accordingly, NMR experiments were conducted under water- and oil-saturated conditions, respectively, to observe the signal characteristics on the transverse relaxation time (T_2) distribution spectra of the two types of pores. The presence of three peaks in the T_2 spectra of lipophilic pores indicates three types of organic pores: volumetrically dominant small pores with short T_2, large pores with long T_2, and microfracture developed in organic matter (Figure 4). Based on the above theoretical understanding, Fu et al. (2021) proposed a method for calculating the proportion of organic and inorganic pores based on the wettability of shale pores.

The calculation results show that the NMR T_2 spectrum of the 1st Section mixed argillaceous shale (M) at saturated oil exhibits doublet characteristics, and the amplitude of the T_2 spectrum at saturated oil is low. The average proportion of organic pores is only 8%, and that of inorganic pores is about 81%. The NMR T_2 spectrum of 2nd Section argillaceous shale (CM) at saturated oil is singlet, the amplitude of the T_2 spectrum at saturated oil is high, and the average proportion of organic pores is more than 14%. The T_2 spectrum of the 3rd Section argillaceous shale (CM) at saturated oil exhibits a singlet shape. The amplitude of the T_2 spectrum at saturated oil is high, but that of saturated water is much higher than that of saturated oil; therefore, the proportion of organic pores is only about 10%. The NMR T_2 spectrum of the 4th Section argillaceous shale (CM) at saturated oil exhibits singlet characteristics, and the average proportion of organic pores exceeds 12% (Figure 5).

4.3 Pore structure quantitative characteristics

4.3.1 N_2 adsorption-desorption isotherms and pore geometry

According to the IUPAC isothermal adsorption curve classification (Thommes et al., 2015), the hysteresis loops of the 1st Section mixed shale (M) are similar to the H4 type (Figure 6A). Furthermore, the adsorption curve is slow near the saturated vapor pressure, reflecting a small amount of gas adsorption, and slit-shaped pores are developed within this section. Hysteresis loops of the 2nd Section argillaceous shale (CM) exhibit the morphologies of both H3 and H4 (Figure 6B), and the gas adsorption amount is small. However, the desorption curves of some samples are steep near the median pressure, forming a wide hysteresis loop, indicating the development of parallel plate-shaped pores. Hysteresis loops of the 3rd Section argillaceous shale (CM) are similar to the H4 type (Figure 6C), and the adsorption curve is slow

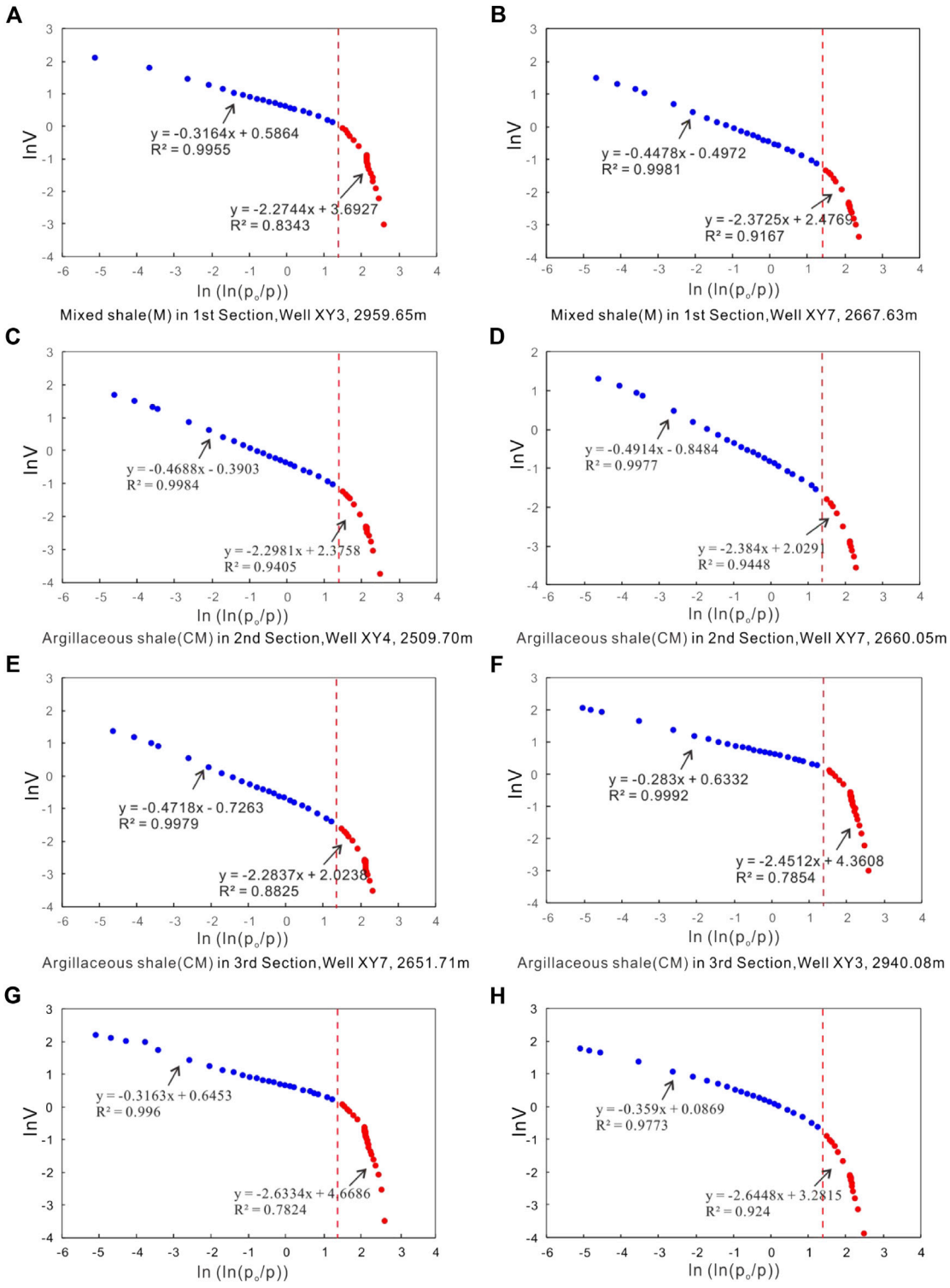

FIGURE 8
Schematic diagram of fractal fitting of shale samples with different lithofacies for the Jurassic Dongyuemiao lacustrine shale in Eastern Sichuan Basin.

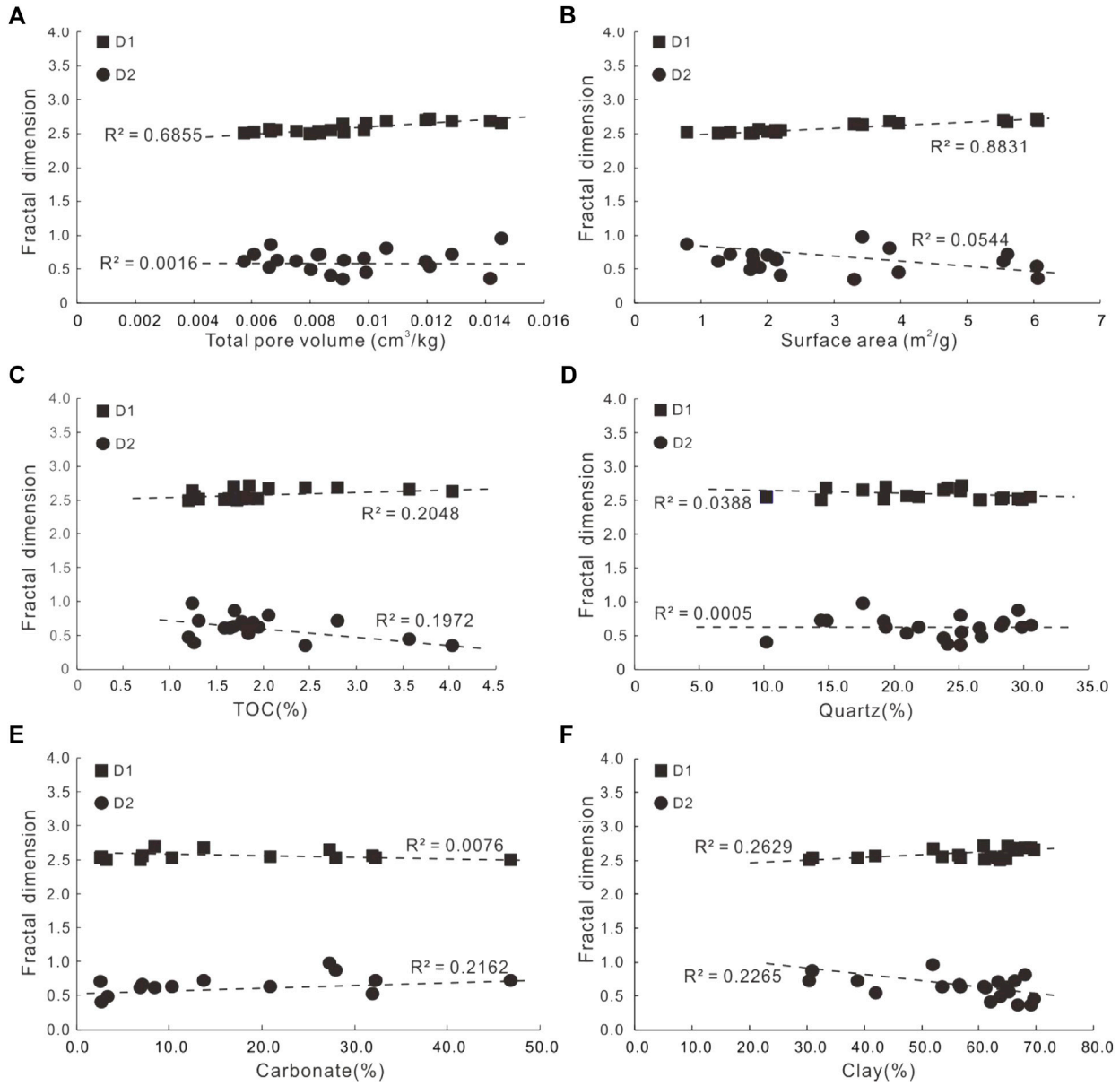

FIGURE 9
Correlations between fractal dimensions, total pore volume, surface area, TOC, quartz content, carbonate content and clay content for the Jurassic Dongyuemiao lacustrine shale in Eastern Sichuan Basin.

near the saturated vapor pressure, suggesting that the gas adsorption amount is small and that the pores are dominated by slit-shaped pores. The hysteresis loops of the 4th Section argillaceous shale (CM) are similar to the H3 type (Figure 6D), and the adsorption curve is steep near the saturated vapor pressure, suggesting a large amount of gas adsorption. The corresponding desorption curve is relatively flat at the median pressure, forming relatively wide hysteresis loops. This suggests that the pores are dominated by parallel plate-shaped pores.

4.3.2 Surface area and pore volume

The SA of the Dongyuemiao lacustrine shale samples were calculated according to the BET model. The SA range of the 1st Section mixed shale (M) is between 0.78 and 5.60 m2/g and that of the 2nd Section argillaceous shale (CM) is between 1.25 and 3.83 m2/g. The SA range of the 3rd Section argillaceous shale (CM) is between 1.43 and 6.04 m2/g and that of the 4th Section argillaceous shale (CM) is between 1.87 and 6.05 m2/g.

The PV of the Dongyuemiao lacustrine shale samples range from 5.73 to 14.54 cm^3/kg, with an average of 9.35 cm^3/kg. The average PV of the 1st Section mixed shale (M) and 3rd Section argillaceous shale (CM) was lower than that of the 2nd Section argillaceous shale (CM) and 4th Section argillaceous shale (CM).

4.3.3 Pore-size distribution

The PSD was characterized by integrating MICP and LTNA experiments. The results show that although the curve morphologies of different samples exhibit slightly differences, the distribution ranges of the pore peaks are similar. The PSD curves of the 2nd, 3rd, and 4th Section argillaceous shale (CM) are characterized by four peaks: 1–2 nm, 20–50 nm, 1,000–1,200 nm, and 10,000–12000 nm (Figure 7).

5 Discussion

In this study, the main controlling factors of pore structure are discussed by correlating fractal dimension with reservoir and pore structure parameters. The surface fractal dimension is denoted as D_1 for relative N_2 pressure $P/P_o > 0.5$ with capillary condensation and surface fractal dimension is denoted as D_2 for $P/P_o < 0.5$ with mono- and multi-layer adsorption (Figure 8).

For lacustrine shale samples, the fractal dimension D_1 represents the development degree of micropores. D_1 is generally larger than D_2 and is closer to 3, suggesting that the pore structure heterogeneity of mesopore-macropore is stronger than that of micropore. A clear positive correlation exists between D_1 and PV as well as SA (Figures 9A,B), indicating that the micropores within the Dongyuemiao lacustrine shale are the main contributors of PV and SA. The correlation between D_1 and TOC is slightly positive, suggesting that the enrichment of organic matter positively affects micropore formation (Figure 9C). Moreover, the enrichment of organic matter does not influence the mesopore–macropore development. Due to the low content of quartz in Dongyuemiao, which is mainly detrital quartz, it does not significantly affect the formation of micropores and mesopore–macropore (Figure 9D). A slight positive correlation exists between D_2 and carbonate content, indicating that intraparticle pores within calcite particles constitute part of mesopore–macropore but not micropores (Figure 9E). Clay minerals are conducive to micropore formation (Figure 9F), but play a negative role in mesopore–macropore formation due to the filling of clay minerals in the mesopore–macropore (Figure 3).

6 Conclusion

1) The 1st and 2nd Sections of Jurassic Dongyuemiao lacustrine shale in Eastern Sichuan Basin are composed of mixed shale lithofacies (M) and argillaceous shale lithofacies (CM). In comparison, the predominant lithofacies of the 3rd Section is argillaceous shale lithofacies (CM). Moreover, the 4th Section constitutes mixed shale lithofacies (M) and argillaceous shale lithofacies (CM).
2) Organic pores (primary pores within plant debris and secondary pores within bitumen), inorganic pores (interparticle pore, intercrystalline pore, and intraparticle pore), and microfractures are present in the Jurassic Dongyuemiao lacustrine shale of Eastern Sichuan Basin. The average proportion of organic pores is higher in the 2nd and 4th Sections, exceeding 12%. The 4th Section, characterized by high organic pore proportion, large amounts of gas adsorption, and parallel plate-shaped pore morphology, exhibits the best pore structure.
3) The micropores within the Dongyuemiao lacustrine shale are the main contributors of PV and SA. The enrichment of organic matter positively affects micropore formation but has no influence on mesopore–macropore development. Additionally, quartz does not significantly affect the formation of nanoscale pores. Intraparticle pores within calcite particles constitute part of mesopore–macropore but not micropores. Clay minerals are conducive to micropore formation but play a negative role in mesopore–macropore development.

Data availability statement

The raw data supporting the conclusion of this article will be made available by the authors, without undue reservation.

Author contributions

YZ contributed as the major author of the article. DH and ZW conceived the project. ZW and XW collected the samples. RL, DW, and YJ analyzed the samples. All authors contributed to the article and approved the submitted version.

Funding

This study was financially supported by the National Natural Science Foundation of China (Grant No. 42272171), National Science and Technology Major Project (Grant No. 2017ZX05036) and Sinopec "Ten Dragons" Technology Project (Grant No. P21078-1).

Conflict of interest

Authors DH, ZW, XW, RL, and DW were employed by Sinopec Exploration Company. The authors YZ, ZW and YJ were employed by PetroChina Key Laboratory of Unconventional Oil and Gas Resources.

The remaining authors declare that the research was conducted in the absence of any commercial or financial relationships that could be construed as a potential conflict of interest.

Publisher's note

All claims expressed in this article are solely those of the authors and do not necessarily represent those of their affiliated organizations, or those of the publisher, the editors and the reviewers. Any product that may be evaluated in this article, or claim that may be made by its manufacturer, is not guaranteed or endorsed by the publisher.

References

Chen, D., Zhang, J., Wang, X., Lan, B., Li, Z., and Liu, T. (2018). Characteristics of lacustrine shale reservoir and its effect on methane adsorption capacity in fuxin basin. *Energy* 32 (11), 11105–11117. doi:10.1021/acs.energyfuels.8b01683

Fan, C., Li, H., Qin, Q., He, S., and Zhong, C. (2020). Geological conditions and exploration potential of shale gas reservoir in Wufeng and Longmaxi Formation of southeastern Sichuan Basin, China. *J. Petroleum Sci. Eng.* 191, 107138. doi:10.1016/j.petrol.2020.107138

Fan, C., Xie, H., Li, H., Zhao, S., Shi, X., Liu, J., et al. (2022). Complicated fault characterization and its influence on shale gas preservation in the southern margin of the Sichuan Basin, China. *Lithosphere* 2022, 8035106. doi:10.2113/2022/8035106

Fu, Y., Jiang, Y., Dong, D., Hu, Q., Lei, Z., Peng, H., et al. (2021). Microscopic pore-fracture configuration and gas-filled mechanism of shale reservoirs in the Western chongqing area, Sichuan Basin, China. *Petroleum Explor. Dev.* 48 (5), 1063–1076. doi:10.1016/S1876-3804(21)60091-5

Gu, Y., Hu, D., Wei, Z., Liu, R., Hao, J., Han, J., et al. (2022b). Sedimentology and geochemistry of the upper permian linghao formation marine shale, central nanpanjiang basin, SW China. *Front. Earth Sci. (Lausanne).* 10, 914426. doi:10.3389/feart.2022.914426

Gu, Y., Li, X., Qi, L., Li, S., Jiang, Y., Fu, Y., et al. (2022a). Sedimentology and geochemistry of the lower permian shanxi formation Shan 2^3 submember transitional shale, eastern Ordos Basin, North China. *Front. Earth Sci. (Lausanne).* 10, 859845. doi:10.3389/feart.2022.859845

Han, H., Dai, J., Guo, C., Zhong, N., Pang, P., Ding, Z., et al. (2021). Pore characteristics and factors controlling lacustrine shales from the upper cretaceous Qingshankou Formation of the Songliao Basin, northeast China: A study combining SEM, low-temperature gas adsorption and MICP experiments. *Acta Geol. sinica-Engl. Ed.* 95 (2), 585–601. doi:10.1111/1755-6724.14419

Han, S., Zhang, J., Brian, H., Jiang, S., Li, W., Chen, Q., et al. (2013). Pore types and characteristics of shale gas reservoir: A case study of lower paleozoic shale in southeast chongqing. *Earth Sci. Front.* 20 (3), 247–253.

Jia, A., Hu, D., He, S., Guo, X., Hou, Y., Wang, T., et al. (2020). Variations of pore structure in organic-rich shales with different lithofacies from the jiangdong Block, fuling shale gas field, SW China: Insights into gas storage and pore evolution. *Energy* 34, 12457–12475. doi:10.1021/acs.energyfuels.0c02529

Li, H. (2022). Research progress on evaluation methods and factors influencing shale brittleness: A review. *Energy Rep.* 8, 4344–4358. doi:10.1016/j.egyr.2022.03.120

Li, J., Jin, W., Wang, L., Wu, Q., Lu, J., and Hao, S. (2016). Quantitative evaluation of organic and inorganic pore size distribution by NMR: A case from the silurian longmaxi formation gas shale in fuling area, Sichuan Basin. *Oil Gas Geol.* 37 (1), 129–134. doi:10.11743/ogg20160118

Li, J., Li, H., Yang, C., Wu, Y., Gao, Z., and Jiang, S. (2022). Geological characteristics and controlling factors of deep shale gas enrichment of the Wufeng-Longmaxi Formation in the southern Sichuan Basin, China. *Lithosphere* 2022, 4737801. doi:10.2113/2022/4737801

Li, P., Liu, Z., Nie, H., Liang, X., Li, Q., and Wang, P. (2021). Heterogeneity characteristics of lacustrine shale oil reservoir under the control of lithofacies: A case study of the Dongyuemiao member of jurassic ziliujing formation, Sichuan Basin. *Front. Earth Sci. (Lausanne).* 9, 736544. doi:10.3389/feart.2021.736544

Liu, Z., Hu, Z., Liu, G., Liu, Z., Liu, H., Hao, J., et al. (2021). Pore characteristics and controlling factors of continental shale reservoirs in the Lower Jurassic Ziliujing Formation, northeastern Sichuan Basin. *Oil Gas Geol.* 42 (1), 136–145. doi:10.11743/ogg20210112

Loucks, R. G., Reed, R. M., Ruppel, S. C., and Hammes, U. (2012). Spectrum of pore types and networks in mudrocks and a descriptive classification for matrix-related mudrock pores. *Am. Assoc. Pet. Geol. Bull.* 96 (6), 1071–1098. doi:10.1306/08171111061

Peng, J., Hu, Z., Feng, D., and Wang, Q. (2022). Sedimentology and sequence stratigraphy of lacustrine deep-water fine-grained sedimentary rocks: The lower jurassic Dongyuemiao Formation in the Sichuan Basin, western China. *Mar. Petroleum Geol.* 146, 105933. doi:10.1016/j.marpetgeo.2022.105933

Qiu, Z., and He, J. (2022). Depositional environment changes and organic matter accumulation of Pliensbachian-Toarcian lacustrine shales in the Sichuan basin, SW China. *J. Asian Earth Sci.* 232, 105035. doi:10.1016/j.jseaes.2021.105035

Rouquerol, J., Avnir, D., Fairbridge, C. W., Everett, D. H., Haynes, J. H., Pernicone, N., et al. (1994). Recommendations for the characterization of porous solids (Technical Report). *Pure Appl. Chem.* 66, 1739–1758. doi:10.1351/pac199466081739

Shu, Y., Bao, H., Zheng, Y., Chen, M., Lu, Y., Liu, H., et al. (2021). Lithofacies types, assemblage characteristics, and sedimentary evolution model of lacustrine shale in Dongyuemiao Formation of Fuxing Area. *Front. Earth Sci. (Lausanne).* 9, 772581. doi:10.3389/feart.2021.772581

Shu, Z., Zhou, L., Li, X., Liu, H., Zeng, Y., Xie, H., et al. (2021). Geological characteristics of gas condensate reservoirs and their exploration and development prospect in the Jurassic continental shale of the Dongyuemiao Member of Ziliujing Formation, Fuxing area, eastern Sichuan Basin. *Oil Gas Geol.* 42 (1), 212–223. doi:10.11743/ogg20210118

Sun, W., Feng, Y., Jiang, C., and Chu, W. (2015). Fractal characterization and methane adsorption features of coal particles taken from shallow and deep coalmine layers. *Fuel* 155, 7–13. doi:10.1016/j.fuel.2015.03.083

Sun, Y., Jiang, Y., Xiong, X., Li, X., Li, S., Qiu, Z., et al. (2022). Lithofacies and sedimentary environment evolution of the $Shan_2^3$ Submember transitional shale of the Shanxi Formation in the Danilng-Jixian area, eastern Ordos Basin. *Coal Geol. Explor.* 50 (9), 104–114. doi:10.12363/issn.1001-1986.21.12.0821

Thommes, M., Kaneko, K., Neimark, A. V., Olivier, J. P., Rodriguez-Reinoso, F., Rouquerol, J., et al. (2015). Physisorption of gases, with special reference to the evaluation of surface area and pore size distribution (IUPAC Technical Report). *Pure Appl. Chem.* 87, 1051–1069. doi:10.1515/pac-2014-1117

Tinni, A., Odusina, E., and Sulucamain, I. (2014). "NMR response of brine, oil, and methane in organic rich shales," in SPE USA Unconventional Resources Conference: The Woodlands, Texas, USA, 1-3 April 2013, 98–106.

Wang, M., Xue, H., Tian, S., Wilkins, R. W. T., and Wang, Z. (2015). Fractal characteristics of upper cretaceous lacustrine shale from the Songliao Basin, NE China. *Mar. Petroleum Geol.* 67, 144–153. doi:10.1016/j.marpetgeo.2015.05.011

Wang, Z., Guo, B., Jiang, C., Qi, L., Jiang, Y., Gu, Y., et al. (2022). Nanoscale pore characteristics of the lower permian shanxi formation transitional facies shale, eastern Ordos Basin, North China. *Front. Earth Sci. (Lausanne).* 10, 842955. doi:10.3389/feart.2022.842955

Wei, G., Wang, W., Feng, L., Tan, X., Yu, C., Zhang, H., et al. (2021). Geological characteristics and exploration prospect of black shale in the Dongyuemiao member of lower jurassic, the eastern Sichuan Basin, China. *Front. Earth Sci. (Lausanne).* 9, 765568. doi:10.3389/feart.2021.765568

Xu, Q., Liu, B., Ma, Y., Song, X., Wang, Y., and Chen, Z. (2017). Geological and geochemical characterization of lacustrine shale: A case study of the jurassic Da'anzhai member shale in the central Sichuan Basin, southwest China. *J. Nat. Gas Sci. Eng.* 47, 124–139. doi:10.1016/j.jngse.2017.09.008

Yang, R., Hu, Q., Yi, J., Zhang, B., He, S., Guo, X., et al. (2019). The effects of mineral composition, TOC content and pore structure on spontaneous imbibition in Lower Jurassic Dongyuemiao shale reservoirs. *Mar. Petroleum Geol.* 109, 268–278. doi:10.1016/j.marpetgeo.2019.06.003

Yang, Z., and Zou, C. (2019). Exploring petroleum inside source kitchen": Connotation and prospects of source rock oil and gas. *Petroleum Explor. Dev.* 46 (1), 181–193. doi:10.1016/S1876-3804(19)30018-7

Zhang, K., Jia, C., Song, Y., Jiang, S., Jiang, Z., Wen, M., et al. (2020a). Analysis of lower cambrian shale gas composition, source and accumulation pattern in different tectonic backgrounds: A case study of weiyuan Block in the upper Yangtze region and xiuwu basin in the lower Yangtze region. *Fuel* 263, 115978. doi:10.1016/j.fuel.2019.115978

Zhang, K., Jiang, Z., Song, Y., Jia, C., Yuan, X., Wang, X., et al. (2022a). Quantitative characterization for pore connectivity, pore wettability, and shale oil mobility of terrestrial shale with different lithofacies-A case study of the Jurassic Lianggaoshan Formation in the Southeast Sichuan Basin of the Upper Yangtze Region in Southern China. *Front. Earth Sci. (Lausanne).* 10, 864189. doi:10.3389/feart.2022.864189

Zhang, K., Peng, J., Liu, W., Li, B., Xia, Q., Cheng, S., et al. (2020b). The role of deep geofluids in the enrichment of sedimentary organic matter: A case study of the late ordovician-early silurian in the upper Yangtze region and early cambrian in the lower Yangtze region, south China. *Geofluids* 2020, 1–12. doi:10.1155/2020/8868638

Zhang, K., Song, Y., Jia, C., Jiang, Z., Han, F., Wang, P., et al. (2022b). Formation mechanism of the sealing capacity of the roof and floor strata of marine organic-rich shale and shale itself, and its influence on the characteristics of shale gas and organic matter pore development. *Mar. Petroleum Geol.* 140, 105647. doi:10.1016/j.marpetgeo.2022.105647

Zhang, K., Song, Y., Jiang, S., Jiang, Z., Jia, C., Huang, Y., et al. (2019). Mechanism analysis of organic matter enrichment in different sedimentary backgrounds: A case study of the lower cambrian and the upper ordovician-lower silurian, in Yangtze region. *Mar. Petroleum Geol.* 99, 488–497. doi:10.1016/j.marpetgeo.2018.10.044

Zhang, K., Song, Y., Jiang, Z., Yuan, X., Wang, X., Han, F., et al. (2022c). Research on the occurrence state of methane molecules in post-mature marine shales-A case analysis of the Lower Silurian Longmaxi Formation shales of the upper Yangtze region in Southern China. *Front. Earth Sci.* 10, 864279. doi:10.3389/feart.2022.864279

Zou, C., Zhu, R., Chen, Z., Ogg, J. G., Wu, S., Dong, D., et al. (2019). Organic-matter-rich shales of China. *Earth. Sci. Rev.* 189, 51–78. doi:10.1016/j.earscirev.2018.12.002